Heavy quark diffusion from coherent color fields in relativistic heavy-ion collisions

Taesoo Song[1,*] and Thomas Epelbaum[2,†]

[1]*Frankfurt Institute for Advanced Studies and Institute for Theoretical Physics, Johann Wolfgang Goethe Universität, Frankfurt am Main, Germany*

[2]*McGill University, Department of Physics 3600 rue University, Montréal QC H3A 2T8, Canada*

The diffusion coefficients of heavy quarks from the coherent color electromagnetic fields which are generated in the early stage of relativistic heavy-ion collisions are calculated at midrapidity, and compared with those obtained from collisions within a thermalized quark-gluon plasma. The coherent color fields are modeled such that they are initially longitudinal and then become isotropic. We found that the diffusion coefficients from the coherent color fields are larger than those from collisions except for very fast heavy quarks, and the color fields are less effective for heavy-quark energy loss. The importance of coherent color fields for heavy-quark diffusion decreases as energy density decreases.

PACS numbers: 25.75.Nq, 25.75.Ld

arXiv:1512.05625v1 [nucl-th] 17 Dec 2015

I. INTRODUCTION

The color glass condensate (CGC) is one of the promising models meant to describe the initial state of relativistic heavy-ion collisions. The model is so named, because the nuclei participating in ultra-relativistic heavy-ion collisions are composed of color fields which slowly evolve with time and are highly occupied.

As the nucleus energy increases, the number of gluons in the nucleus rapidly increases while the cross section for the nucleus scattering slowly increases. This implies that the gluon fields in the nucleus are highly occupied at high energy, and should be saturated by nonlinear interactions. Due to the high density, the distance between gluons is so short that the strong coupling strength is in fact small. However, the gluon interactions are coherent and become strong as the gravitational interactions do [1].

In extremely high energy collisions, the nucleus is like an infinitely thin sheet of color glass. Partons with large energy fractions in the nucleus play the role of color sources, and those with small energy fractions are described as the classical color fields generated by the sources. The color sources are distributed on the color sheet with the transverse size of the order of the inverse saturation momentum, and the color electromagnetic fields have only transverse components before heavy-ion collision.

Rapidity dependence ignored, one can numerically calculate color fields in space-time by solving the classical Yang-Mills equations. At the contact time of two color sheets, longitudinal color electromagnetic fields are instantaneously generated in forward light cone, and then transverse color electromagnetic fields grow till they are comparable to the longitudinal ones [2, 3]. One cannot reach isotropic color electromagnetic fields only by solving the classical Yang-Mills equations, and quantum corrections seem to be needed [4]. The nuclear matter between the two color glasses before the formation of an isotropic quark-gluon plasma (QGP) is called the glasma.

Heavy flavor is one of the important probes in search of the properties of the hot dense nuclear matter created in relativistic heavy-ion collisions. It has been found that the nuclear modification factor and elliptic flow of heavy flavors are not small in relativistic heavy-ion collisions, which indicates strong interactions of heavy flavors with the hot dense nuclear matter [5–8]. There are numerous theoretical studies to explain experimental data, where heavy flavor interacts with nuclear matter through collision and gluon radiation [9–29].

In the CGC picture, relativistic heavy-ion collision generates strong coherent color fields between two receding heavy nuclei. Since heavy flavor is early produced, it will interact with the strong color fields. The production time of heavy quark pair is at most $1/(2m_Q)$ with m_Q being the heavy quark mass. Considering the masses of charm and bottom quarks being respectively about 1.5 and 5.0 GeV, the production times are less than 0.07 and 0.02 fm/c. They are smaller than the typical time scale during which the CGC model should be valid, especially for the bottom quark. The heavy quark interactions with the strong coherent color fields take place mainly before initial thermalization while collisions or gluon radiations of heavy quarks in QGP, which have been widely studied, take place after that. Since the coherent color fields have a random color and a random direction, the heavy quarks traveling through these fields will diffuse as in a thermalized QGP.

In this study, we calculate the diffusion coefficients of a heavy quark from coherent color fields in relativistic heavy-ion collisions and compare them with those obtained from collisions within a thermalized QGP.

This paper is organized as follows: The diffusion coefficients of heavy flavor induced by color fields are calculated in Sec. II, and they are computed for realistic relativistic heavy-ion collisions in Sec. III. In Sec. IV, these diffusion coefficients are then compared with those

*Electronic address: song@fias.uni-frankfurt.de
†Electronic address: epelbaum@physics.mcgill.ca

obtained from collisions within a thermalized QGP, and a summary is given in Sec. V.

II. DIFFUSION COEFFICIENTS IN COLOR FIELDS

Let us start with the nonrelativistic Langevin equations expressed as [10]

$$\begin{aligned} \frac{dp_L}{dt} &= -\eta_D(p)p + \xi_L, \\ \frac{dp_T}{dt} &= \xi_T, \end{aligned} \tag{1}$$

where p_L and p_T are, respectively, the longitudinal and transverse momenta of a particle, η_D a momentum drag coefficient, and ξ_L and ξ_T random momentum kicks in the longitudinal and transverse directions which satisfy

$$\begin{aligned} \langle \xi_L^i(t)\xi_L^j(t')\rangle &= \kappa_L(p)\hat{p}^i\hat{p}^j\delta(t-t'), \\ \langle \xi_T^i(t)\xi_T^j(t')\rangle &= \kappa_T(p)(\delta^{ij}-\hat{p}^i\hat{p}^j)\delta(t-t'), \\ \langle \xi_T^i(t)\xi_L^j(t')\rangle &= 0, \end{aligned} \tag{2}$$

where $\langle\ldots\rangle$ represents ensemble average, $\kappa_L(p)$ and $\kappa_T(p)$ are the mean-squared longitudinal and transverse momentum transfers per unit time, and $\hat{\mathbf{p}}$ is the unit vector of the particle three-momentum. $\delta(t-t')$ in Eq. (2) implies that the random forces at two different times are completely uncorrelated. However, it is not true in reality, because any force acting on a particle cannot be as sharp as a delta function. One may use a normalized gaussian function with a finite width instead of a delta function. This is the strategy we will adopt in the following. Integrating Eq. (2) over t' leads to

$$\begin{aligned} \kappa_L(p) &= 2\hat{p}_i\hat{p}_j D^{ij}, \\ \kappa_T(p) &= (\delta_{ij}-\hat{p}_i\hat{p}_j)D^{ij}, \end{aligned} \tag{3}$$

where D_{ij} is a diffusion tensor defined as [31]

$$D^{ij} = \frac{1}{2}\int_{-\infty}^{\infty} dt' \langle \xi^i(t')\xi^j(t)\rangle = \int_{-\infty}^{t} dt' \langle \xi^i(t')\xi^j(t)\rangle, \tag{4}$$

where $\xi^i = \xi_L^i + \xi_T^i$ and we have assumed that the correlator is a function of $|t-t'|$, an assumption that makes sense for a thermal bath at constant temperature. We note that the random forces in Eq. (4) do not need the subscript L or T by virtue of the tensor structures in Eq. (3).

Fig. 1 shows schematic cartoons for a heavy quark scattering with initial coherent color fields and within a thermalized QGP in relativistic heavy-ion collisions. Since the initial coherent fields have a random color and a random leftward or rightward direction, with a typical transverse size of the order of the inverse saturation momentum, a heavy quark interaction with the fields is similar

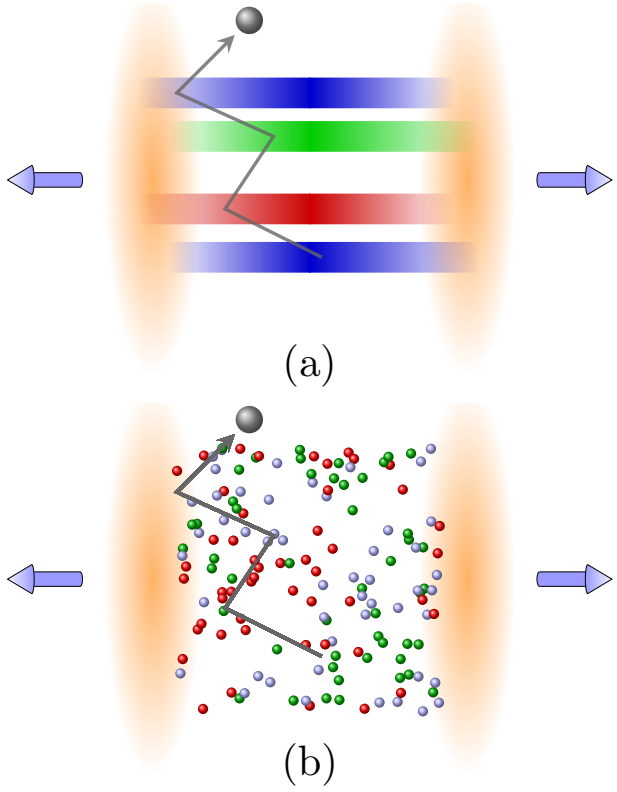

FIG. 1: (Color online) Schematic figures for a heavy quark scattering with initial coherent color fields (a) and within a thermalized QGP (b) in relativistic heavy-ion collisions.

with random scatterings in a thermalized QGP. Therefore, the random force in Eq. (4) can be substituted by the color Lorentz force, $\mathbf{F} = g_s Q^a(\mathbf{E}^a + \mathbf{v}\times\mathbf{B}^a)$ where g_s, Q^a and $\mathbf{v}$ are respectively the strong coupling constant, the charge of color a, and the velocity of a parton in the color electric and magnetic fields, $\mathbf{E}^a$ and $\mathbf{B}^a$. The correlation of the color Lorentz force is then expressed as

$$\begin{aligned} \langle F_i(x')F_j(x)\rangle = g_s^2\frac{C_2\delta^{ab}}{N_c^2-1}\Big[&\langle E_i^a(x')E_j^b(x)\rangle \\ &+\varepsilon_{ikl}\varepsilon_{jmn}v_k v_m\langle B_l^a(x')B_n^b(x)\rangle\Big], \end{aligned} \tag{5}$$

where N_c is the number of colors, $C_2 = 1/2$ for quark and $C_2 = N_c$ for gluon from $Q^aQ^b = C_2\delta^{ab}/(N_c^2-1)$, ε_{ikl} and ε_{jmn} are the usual Levi-Civita antisymmetric tensors, and $\langle E_iB_j\rangle = \langle B_iE_j\rangle = 0$ is assumed [30, 32]. Identifying the color Lorentz force with the medium kicks in Eq. (4) leads to the following expressions for κ_L and

κ_T

$$\kappa_L = \frac{2g_s^2 C_2}{N_c^2-1}\int_{-\infty}^{t} dt' \Big\langle E_L^a(x')E_L^a(x)\Big\rangle,$$
$$\kappa_T = \frac{g_s^2 C_2}{N_c^2-1}\int_{-\infty}^{t} dt' \Big[\Big\langle \vec{E}^a(x')\cdot\vec{E}^a(x)\Big\rangle - \Big\langle E_L^a(x')E_L^a(x)\Big\rangle + \Big\langle \vec{v}(x')\cdot\vec{v}(x)\vec{B}^a(x')\cdot\vec{B}^a(x)\Big\rangle - \Big\langle \vec{v}\cdot\vec{B}^a(x')\vec{v}\cdot\vec{B}^a(x)\Big\rangle\Big], \quad (6)$$

where $E_L \equiv \hat{p}\cdot\vec{E}^a$ is defined as the longitudinal color electric field. As mentioned below Eq. (2), random forces are spread with finite widths in space-time. Therefore, we introduce a Gaussian form for the correlation of color electromagnetic fields at two different space-time:

$$\langle E_i^a(x')E_j^a(x)\rangle = \delta_{ij}\langle E_i^a E_i^a\rangle(x)\exp\left[-\sum_\mu \frac{(x_\mu - x'_\mu)^2}{2\sigma_\mu^2}\right],$$
$$\langle B_i^a(x')B_j^a(x)\rangle = \delta_{ij}\langle B_i^a B_i^a\rangle(x)\exp\left[-\sum_\mu \frac{(x_\mu - x'_\mu)^2}{2\sigma_\mu^2}\right], \quad (7)$$

where σ_μ is the correlation length of color electromagnetic fields in μ direction.

Since we study a heavy quark in coherent color fields, $C_2 = 1/2$, and the velocity does not change much: $\vec{v}(x') \approx \vec{v}(x) \equiv \vec{v}$. Substituting Eq. (7) into Eq. (6), κ_L and κ_T are simplified into

$$\kappa_L = \frac{g_s^2\tau_m}{N_c^2-1}\langle (E_L^a)^2\rangle,$$
$$\kappa_T = \frac{g_s^2\tau_m}{2(N_c^2-1)}\langle (E_T^a)^2 + v^2(B_T^a)^2\rangle, \quad (8)$$

where E_T and B_T are respectively the transverse color electric and magnetic fields, and τ_m is the memory time of the color electromagnetic field defined as

$$\tau_m \equiv \int_{-\infty}^{t} dt' \exp\left[-\sum_\mu \frac{(x_\mu - x'_\mu)^2}{2\sigma_\mu^2}\right] = \int_{-\infty}^{t} dt' \exp\left[-\frac{(t-t')^2}{2\sigma_0^2} - \sum_{i=1,2,3}\frac{v_i^2(t-t')^2}{2\sigma_i^2}\right]. \quad (9)$$

It is interesting to notice that since magnetic fields induce only transverse force, they do not contribute to κ_L in Eq. (8).

For a mid-rapidity heavy quark in relativistic heavy-ion collisions, the memory time is given by

$$\tau_m = \frac{1}{2}\int_{-\infty}^{\infty} dt' \exp\left[-\frac{(t-t')^2}{2}\left\{\frac{1}{\sigma_0^2} + \frac{v_T^2}{\sigma_T^2}\right\}\right] = \sqrt{\frac{\pi}{2}}\left[\frac{1}{\sigma_0^2} + \frac{v_T^2}{\sigma_T^2}\right]^{-1/2}, \quad (10)$$

where v_T and σ_T are, respectively, the transverse velocity of a heavy quark and the transverse correlation length of color electromagnetic fields. In the CGC, the latter is approximately the inverse of saturation momentum, $\sigma_T \simeq 1/Q_s$ [1], which is around 0.1∼0.2 fm at the Relativistic Heavy Ion Collider (RHIC) and the Large Hadron Collider (LHC) energies [33]. Assuming boost invariance, σ_0 is roughly the lifetime of coherent color fields and expected to be larger than σ_T. For a fast heavy quark ($v_T \gg \sigma_T/\sigma_0$), the memory time approximates to

$$\tau_m \simeq \sqrt{\frac{\pi}{2}}(Q_s v_T)^{-1}, \quad (11)$$

and for a slow heavy quark ($v_T \ll \sigma_T/\sigma_0$),

$$\tau_m \simeq \sqrt{\frac{\pi}{2}}\sigma_0. \quad (12)$$

From the Fixed-Order Next-to-Leading Logarithm (FONLL) calculations [34], the average transverse momenta of mid-rapidity charm quarks are respectively 1.5 GeV and 2.4 GeV in p+p collisions at $\sqrt{s_{\rm NN}} = 200$ GeV and 2.76 TeV, which correspond to v_T =0.7 and 0.85. For mid-rapidity bottom quarks, the average transverse velocities are respectively 0.58 and 0.7. Therefore, we take the approximation of Eq. (11) in this study.

III. APPLICATION TO RELATIVISTIC HEAVY-ION COLLISIONS

The CGC model introduces a separation scale x_0: the partons which have larger energy fractions than x_0 are treated as static color sources while those with smaller energy fractions as classical color fields generated by the sources. The color sources are located near the color sheets, which are the Lorentz-contracted nuclei, with a transverse size of the order of the inverse saturation momentum. After two color sheets pass through each other in relativistic heavy-ion collisions, the classical color fields are calculated in forward light cone by numerically solving the classical Yang-Mills equations, satisfying the boundary conditions given by color sources on the light cone [2, 3]. The numerical calculations assume boost invariance, which means that the physics does not depend on $\eta \sim \ln[(t+z)/(t-z)]$. Though it seems similar to the capacitor problem in electrodynamics, color sources are randomly distributed on the sheet with a characteristic transverse size, and nonabelian gauge equations are to be solved. The results show that longitudinal color electric and magnetic fields are instantaneously generated at the contact time of two color sheets, and then they diminish with time. On the other hand, transverse color electric and magnetic fields, which are initially absent in forward light cone, grow with time till they are comparable to longitudinal ones in strength [2, 3]. In other words, the

initial color electromagnetic fields are given by

$$(E_z^a)^2 \simeq (B_z^a)^2 \neq 0, \quad E_{x,y}^a = B_{x,y}^a = 0, \tag{13}$$

and the asymptotic final ones by

$$(E_z^a)^2 \simeq (E_x^a)^2 + (E_y^a)^2, \quad (B_z^a)^2 \simeq (B_x^a)^2 + (B_y^a)^2, \tag{14}$$

and more details can be found in Appendix B. From the energy-momentum tensor of pure gauge Quantum Chromodynamics (QCD) Lagrangian,

$$T_{\mu\nu} = \frac{1}{4} g_{\mu\nu} F^{\alpha\beta a} F^a_{\alpha\beta} - g^{\alpha\beta} F^a_{\mu\alpha} F^a_{\nu\beta}, \tag{15}$$

energy density and pressure are, respectively, given by

$$\varepsilon = T_{00} = \frac{1}{2}\left\{ (E^a)^2 + (B^a)^2 \right\}, \quad p_i = T_{ii} = \varepsilon - E_i^{a2} - B_i^{a2}, \tag{16}$$

where $i = 1 \sim 3, E_i^a = F_{0i}^a$ and $B_i^a = -(1/2)\epsilon_{ijk} F^{ajk}$. Substituting Eq. (13) and (14) into Eq. (16), initial pressures are given by

$$p_x = p_y = \varepsilon, \quad p_z = -\varepsilon, \tag{17}$$

and final ones by

$$p_x = p_y = \varepsilon/2, \quad p_z = 0. \tag{18}$$

Since the initial color fields are expected to eventually turn into isotropic gluon gas, it seems that the classical Yang-Mills equations are not sufficient, and quantum corrections are needed in order for the complete time-evolution of initial gluonic matter to show signs of isotropization [4].

In order to deal with the anisotropic pressure, we introduce a parameter defined by $\zeta \equiv p_z/p_x \simeq p_z/p_y$. The squared color electric fields are then expressed as

$$(E_x^a)^2 + (E_y^a)^2 = \frac{\zeta+1}{\zeta+2}(E^a)^2, \quad (E_z^a)^2 = \frac{1}{\zeta+2}(E^a)^2, \tag{19}$$

and same for color magnetic fields. We note that $\zeta = -1$ at the contact time of two color sheets, and ζ should evolve towards $+1$, which corresponds to isotropic color fields. In practice, ζ converges towards 0 (free-streaming) for the late time behavior of classical Yang-Mills evolution with classical initial conditions.

From Eq. (19), the longitudinal and transverse components of color electromagnetic fields for a mid-rapidity heavy quark which moves in transverse (x, y) direction are respectively given by

$$\langle (E_L^a)^2 \rangle = \frac{\zeta+1}{2(\zeta+2)} \langle (E^a)^2 \rangle, \quad \langle (E_T^a)^2 \rangle = \frac{\zeta+3}{2(\zeta+2)} \langle (E^a)^2 \rangle, \tag{20}$$

and the same equations for color magnetic fields. Substituting Eq. (11) and (20) into Eq. (8),

$$\kappa_L = \frac{\sqrt{2}\pi^{3/2}\alpha_s}{(N_c^2-1)Q_s} \frac{\zeta+1}{\zeta+2} \left\langle \frac{(E^a)^2}{v} \right\rangle, \quad \kappa_T = \frac{\pi^{3/2}\alpha_s}{\sqrt{2}(N_c^2-1)Q_s} \frac{\zeta+3}{\zeta+2} \left\langle \frac{(E^a)^2}{v} + v(B^a)^2 \right\rangle, \tag{21}$$

where $\alpha_s = g_s^2/(4\pi)$. From the relation $(E^a)^2 = (B^a)^2 = \varepsilon$ derived in appendix A, Eq. (21) is finally expressed in term of the energy density as:

$$\kappa_L = \frac{\sqrt{2}\pi^{3/2}\alpha_s\varepsilon}{(N_c^2-1)Q_s} \frac{\zeta+1}{\zeta+2} v^{-1}, \quad \kappa_T = \frac{\pi^{3/2}\alpha_s\varepsilon}{\sqrt{2}(N_c^2-1)Q_s} \frac{\zeta+3}{\zeta+2} \left(\frac{1}{v} + v \right). \tag{22}$$

It seems that Eq. (22) diverges for a static heavy quark. In this case, however, one should use Eq. (12) for memory time instead of Eq. (11).

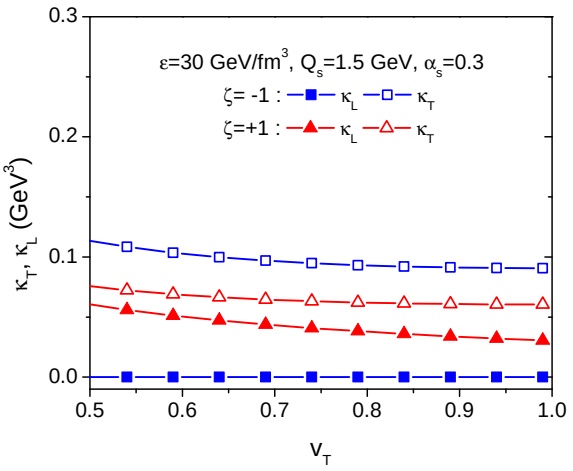

FIG. 2: (Color online) κ_L (filled) and κ_T (open) of a mid-rapidity heavy quark from the initial (blue) and isotropic (red) coherent color fields, which correspond to $\zeta = -1$ and $\zeta = +1$ respectively. Energy density, the saturation momentum, and α_s are, respectively, taken to be 30 GeV/fm^3, 1.5 GeV, and 0.3.

Fig. 2 shows κ_L and κ_T of a mid-rapidity heavy quark from initial and isotropic coherent color fields. The energy density, the saturation momentum, and α_s are respectively taken to be 30 GeV/fm^3, 1.5 GeV, and 0.3. Since the initial color electromagnetic fields ($\zeta = -1$)

generate only non-zero z-component of the Lorentz force, κ_L vanishes identically, while κ_T is largest. As ζ increases, κ_L increases while κ_T decreases. In isotropic color fields ($\zeta = +1$), κ_T is still larger than κ_L though, as κ_T receives an additional contribution from color magnetic fields, as seen in Eq. (22).

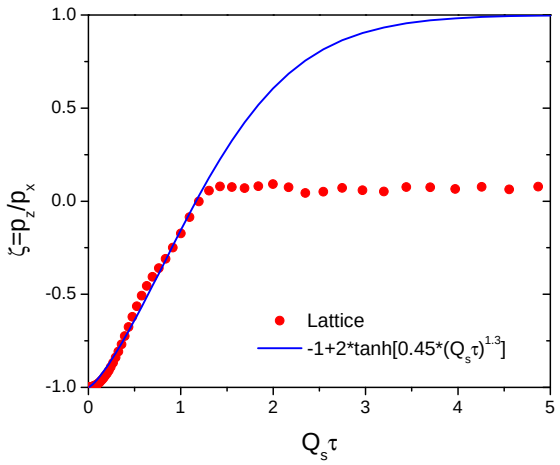

FIG. 3: (Color online) pressure anisotropy ζ as a function of $Q_s\tau$ from the lattice calculations of classical Yang-Mills equations [4] and from a parametrization.

Fig. 3 shows the pressure anisotropy ζ from the lattice calculations of classical Yang-Mills equations [4]. Computations were performed on a 512^2 lattice with the transverse lattice spacing being fixed to $a_T = 1$. As mentioned before, ζ from the classical Yang-Mills equations starts from -1 and saturates around 0. Assuming that complete solutions beyond those of classical Yang-Mills equations lead to $\zeta = +1$ at large $Q_s\tau$, we parameterize

$$\zeta(\tau) = -1 + 2\tanh[0.45(Q_s\tau)^{1.3}], \tag{23}$$

which is shown as a blue line in Fig. 3. The parameterized function reproduces lattice results up to $Q_s\tau \simeq 1.2$ and converses to $\zeta = +1$.

The time-evolution of the energy density is obtained by using Bjorken's law

$$\frac{\partial\varepsilon}{\partial\tau} = -\frac{\varepsilon + p_L}{\tau} = -\frac{2(\zeta+1)}{\zeta+2}\frac{\varepsilon}{\tau} \tag{24}$$

whose solution is

$$\varepsilon(\tau) \sim \tau^{-\frac{2(\zeta+1)}{\zeta+2}}. \tag{25}$$

We note that the energy density is initially constant ($\zeta = -1$), then decreases like free streaming ($\zeta = 0$) and finally isentropically ($\zeta = +1$).

Fig. 4 shows the energy densities as a function of τ in central heavy-ion collisions at RHIC and LHC where Q_s are taken to be respectively 1 and 2 GeV. Initial energy densities $\varepsilon(\tau = 0)$ are rescaled to meet the initial

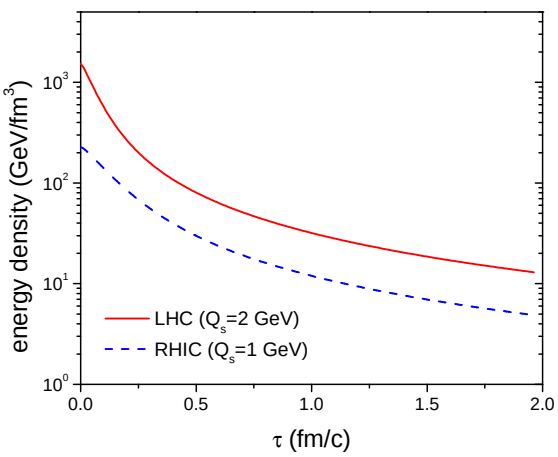

FIG. 4: (Color online) energy densities as a function of τ in central heavy-ion collisions at RHIC and LHC where Q_s are respectively 1 and 2 GeV.

conditions of hydrodynamic simulations around $\tau = 0.5$ fm/c [35].

Then the diffusion coefficients of a heavy quark in relativistic heavy-ion collisions are given from Eq. (6) by

$$\kappa_L(\tau, v) = \frac{2\pi\alpha_s}{N_c^2 - 1}\int_{\tau_0}^{\tau} d\tau'\varepsilon(\tau')\frac{\zeta(\tau')+1}{\zeta(\tau')+2} \times \exp\left[-\frac{v^2Q_s^2}{2}(\tau-\tau')^2\right], \tag{26}$$

$$\kappa_T(\tau, v) = \frac{\pi\alpha_s}{N_c^2 - 1}\int_{\tau_0}^{\tau} d\tau'\varepsilon(\tau')\frac{\zeta(\tau')+3}{\zeta(\tau')+2} \times(1+v^2)\exp\left[-\frac{v^2Q_s^2}{2}(\tau-\tau')^2\right]. \tag{27}$$

where the heavy quark production time $\tau_0 = 1/(2M_T)$ with M_T being the transverse mass of heavy quark.

Fig. 5 shows κ_L and κ_T of a mid-rapidity heavy quark as a function of the heavy-quark velocity at $\tau = 0.5$ fm/c in central Au+Au collisions at $\sqrt{s_{\rm NN}}$ =200 GeV. Q_s and α_s are respectively taken to be 1 GeV and 0.3. We can see that the κ_T of bottom quark is larger than that of charm quark due to the smaller production time τ_0 of bottom quark in Eq. (27). Since the production times of both charm and bottom quarks become short for large velocity, the difference of κ_T decreases with increasing heavy quark velocity. On the other hand, the κ_L of bottom quark is similar to that of charm quark regardless of velocity, because κ_L is very small near the production time of heavy quark ($\zeta \approx -1$).

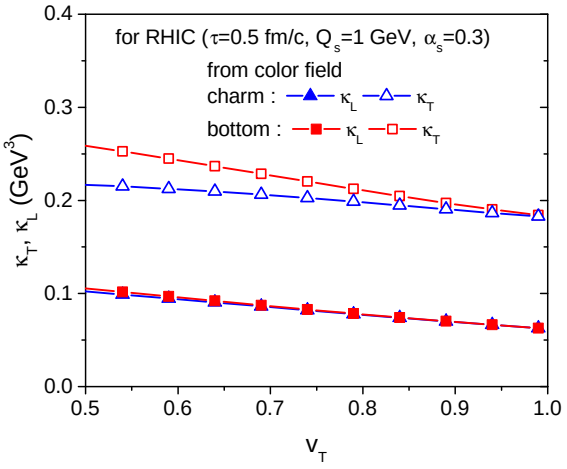

FIG. 5: (Color online) κ_L (filled) and κ_T (open) of a mid-rapidity charm (triangle) and bottom (square) quarks as a function of heavy-quark velocity at $\tau = 0.5$ fm/c in central Au+Au collisions at $\sqrt{s_{\rm NN}}$ =200 GeV. Q_s and α_s are respectively taken to be 1 GeV and 0.3.

IV. COMPARISON WITH THE DIFFUSION COEFFICIENTS INDUCED BY COLLISIONS

As the system expands, the initial color fields become more and more dilute, and they can start to be described by individual quanta, that is, gluons. In this section, we compare κ_L and κ_T of heavy quarks from coherent color fields with those induced by collisions within a thermalized quark-gluon plasma (QGP) at the same energy density.

Since the initial nuclear matter in relativistic heavy-ion collisions is highly occupied, the interspace between color quanta is short and perturbative QCD (pQCD) is applicable. To the leading order in pQCD, κ_L and κ_T of heavy quark from collision read as followings [10]:

$$\kappa_L = \frac{4\pi C_H \alpha_s^2 T^3}{3}\left(\frac{1}{v^2} - \frac{1-v^2}{2v^3}\ln\frac{1+v}{1-v}\right)$$
$$\times\left\{N_c[\ln(T/m_D) + C_b(v)] + \frac{N_f}{2}[\ln(T/m_D) + C_f(v)]\right\},$$
$$\kappa_T = \frac{4\pi C_H \alpha_s^2 T^3}{3}\left(\frac{3}{2} - \frac{1}{2v^2} + \frac{(1-v^2)^2}{4v^3}\ln\frac{1+v}{1-v}\right)$$
$$\times\left\{N_c[\ln(T/m_D) + B_b(v)] + \frac{N_f}{2}[\ln(T/m_D) + B_f(v)]\right\}, \quad (28)$$

where $C_H = (N_c^2-1)/(2N_c)$, N_f is the number of light flavors, $B_b(v)$, $B_f(v), C_b(v)$, and $C_f(v)$ are functions of the heavy quark velocity [10], and m_D is the Debye screening mass, which is taken to be 1.5 T with T being the temperature.

In Fig. 6, red lines with filled and open triangles show, respectively, κ_L and κ_T for collisions at $\tau = 0.5$ fm/c and 1.0 fm/c in central Au+Au collisions at $\sqrt{s_{\rm NN}}$ =200 GeV. Temperatures in Eq. (28) are obtained from

$$\varepsilon = \left(\frac{d_g}{30} + \frac{7d_q}{120}\right)\pi^2 T^4, \quad (29)$$

where $d_g = 16$ and $d_q = 18$ are respectively the degrees of freedom of gluons and of light quarks. Energy densities are 30 GeV/fm^3 and 12 GeV/fm^3, respectively, at $\tau = 0.5$ fm/c and 1.0 fm/c from particle multiplicities in central Au+Au collisions at $\sqrt{s_{\rm NN}}$ =200 GeV [35]. They are compared with κ_L and κ_T from coherent color fields, which are shown as blue lines with filled and open squares. The saturation momentum is taken to be 1.0 GeV, and $\alpha_s = 0.3$ for both collisions and color Lorentz force. Comparing the diffusion coefficients from color fields and those

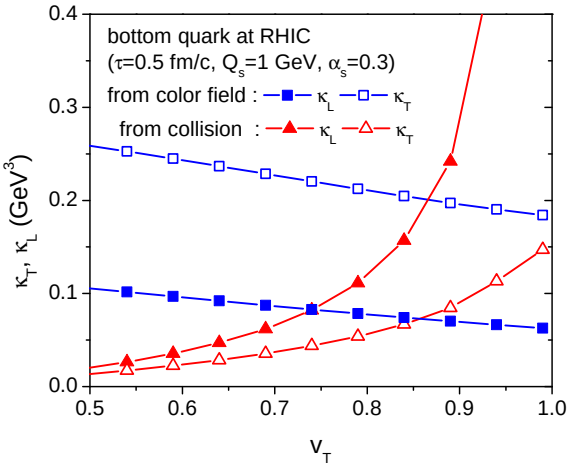

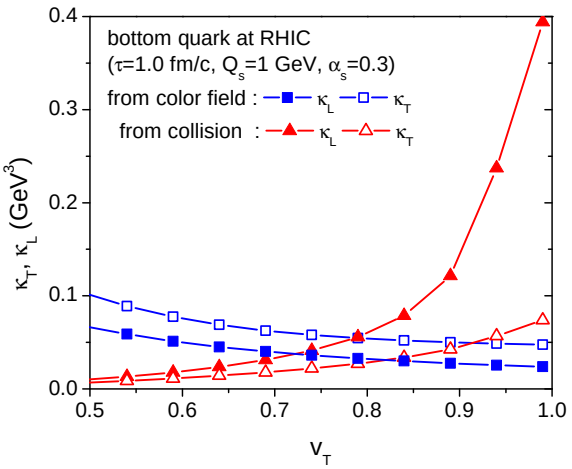

FIG. 6: (Color online) κ_L (filled) and κ_T (open) of a mid-rapidity bottom quark induced by collisions within a thermalized QGP (triangle), and from coherent color fields (square) at $\tau = 0.5$ fm/c (upper) and 1.0 fm/c (lower) in central Au+Au collisions at $\sqrt{s_{\rm NN}}$ =200 GeV [35]. The saturation momentum is taken to be 1.0 GeV, and $\alpha_s = 0.3$ for both collisions and color Lorentz force.

from collisions, we find two qualitative differences:

- Firstly, κ_T from color fields is always larger than κ_L, whereas the opposite relation holds for collisions. Since κ_L is related to the drag coefficient and energy loss of energetic heavy quarks, the coherent color fields are less effective for heavy-quark energy loss when compared to collisions.

- Secondly, κ_L and κ_T from collisions increase with the heavy-quark velocity, while those from color fields decrease. Since fast heavy quarks have more chance of colliding within the QGP and one collision has larger impact on it, κ_L and κ_T from collisions increase with heavy quark velocity. On the other hand, fast heavy quarks remain only during a small amount of time within one color domain of the transverse plane. It thus shortens the memory time defined in Eq (9), and, as a result, κ_L and κ_T from color fields decrease.

In the upper panel of Fig. 6 where $\tau = 0.5$ fm/c, κ_T from the color Lorentz force is larger than the one induced by collisions, and the same holds true for κ_L up to $v = 0.74$. In the lower panel where $\tau = 1.0$ fm/c, however, κ_T from the color Lorentz force is larger up to $v = 0.92$, and κ_L up to $v = 0.72$. This shows that as time increases, the diffusion coefficients from coherent color fields become less important, compared to those induced by collisions in relativistic heavy-ion collisions. There are two reasons for that. In Eq. (27), κ_L and κ_T from color fields are proportional to the energy density, while those from collisions to T^3 or $\varepsilon^{3/4}$ from Eq. (28) and (29). Furthermore, κ_L and κ_T from color fields are proportional to α_s while those induced by collisions to α_s^2. Therefore, coherent color fields are more important for heavy quark diffusion in the initial stage of relativistic heavy-ion collisions, where ε is large and α_s is small. If the saturation momentum decreases, then the transverse size of the color-field domains grows and the effect of coherent color fields becomes stronger for a longer time. Comparing the upper and lower panels of Fig. 6, we also find that κ_L and κ_T from color fields are early overtaken by those induced by collisions for fast heavy quarks, and late overtaken for slow heavy quarks. Assuming that κ_L and κ_T from color fields turn into those induced by collisions as time increases, this suggests that initial coherent color fields are early seen as individual gluons by fast heavy quarks. This seems reasonable, because the density of glasma decreases in the rest frame of fast heavy quarks.

Fig. 7 compares κ_L and κ_T from coherent color fields and those induced by collisions in central Pb+Pb collisions at 2.76 TeV. The saturation momentum and α_s are respectively taken to be 2.0 GeV and 0.3. κ_T from color fields is larger than that from collision up to $v = 0.89$ in the upper panel, and up to $v = 0.79$ in the lower panel. On the other hand, κ_L from color fields is larger than the one induced by collisions up to $v = 0.69$ and $v = 0.64$ in the upper and lower panels respectively. Though energy densities in Pb+Pb collisions at $\sqrt{s_{\rm NN}}$ =2.76 TeV are higher than in Au+Au collisions at $\sqrt{s_{\rm NN}}$ =200 GeV, coherent color fields play a less important roles in heavy quark diffusion due to a larger saturation momentum.

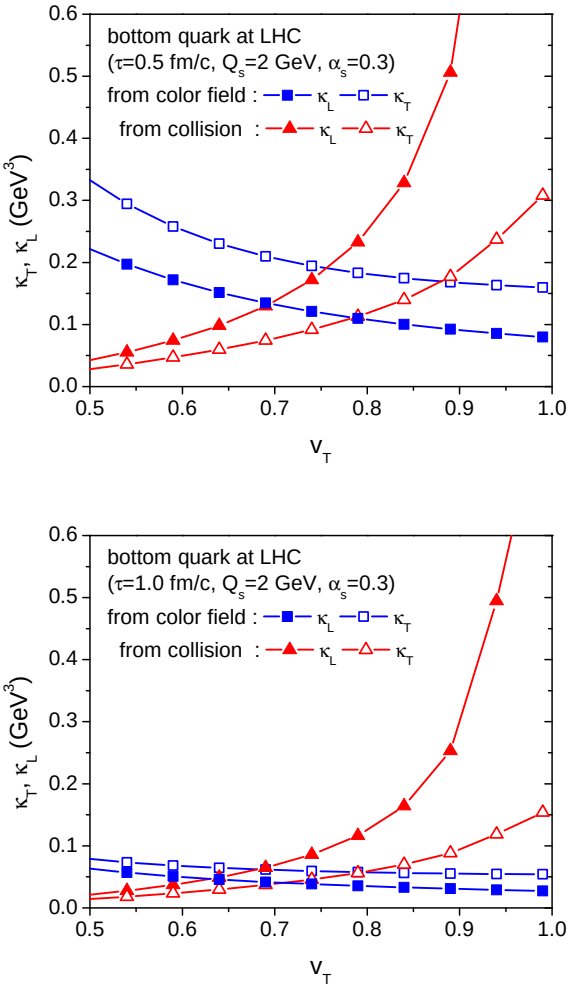
bottom quark at LHC
(τ=0.5 fm/c, Q_s=2 GeV, α_s=0.3)
from color field : κ_L κ_T
from collision : κ_L κ_T
κ_T, κ_L (GeV^3)
v_T
bottom quark at LHC
(τ=1.0 fm/c, Q_s=2 GeV, α_s=0.3)
from color field : κ_L κ_T
from collision : κ_L κ_T
κ_T, κ_L (GeV^3)
v_T

FIG. 7: (Color online) κ_L (filled) and κ_T (open) of a mid-rapidity bottom quark from collisions within thermalized QGP (triangle), and from coherent color fields (square) at $\tau = 0.5$ fm/c (upper) and 1.0 fm/c (lower) in central Pb+Pb collisions at $\sqrt{s_{\rm NN}}$ =2.76 TeV [36]. The saturation momentum and α_s are respectively taken to be 2.0 GeV and 0.3 in both panels.

V. SUMMARY

Heavy quark is a promising probe for the properties of the hot dense nuclear matter created in relativistic heavy-ion collisions. Though the interactions of heavy quarks with thermalized hot dense nuclear matter have been extensively studied, the interactions before thermal equilibrium has been reached in relativistic heavy-ion collisions

have barely been studied. According to the CGC model, the initial nuclear matter is composed of strong coherent color fields, which are initially highly anisotropic and then presumably evolve towards an isotropic gluon gas.

In this study we have calculated the diffusion coefficients of heavy quarks induced by interactions with coherent color fields. Due to our lack of knowledge of the correlation length of the color fields in τ and η directions, our calculations were restricted to mid-rapidity heavy quarks with rather large velocities. The coherent color fields were modeled such that they initially follow the numerical results from lattice calculations and then finally become isotropic.

We then compared the diffusion coefficients with those obtained from collisions within a thermalized QGP in Au+Au collisions at $\sqrt{s_{\rm NN}}$ =200 GeV, and in Pb+Pb collisions at $\sqrt{s_{\rm NN}}$ =2.76 TeV. From this comparison, we have found a couple of qualitative differences between diffusion coefficients from color fields and those from collisions:

- Firstly, κ_T calculated from interactions with color fields is always larger than κ_L for a mid-rapidity heavy quark in relativistic heavy-ion collisions, which is opposite to the conclusion one draws from collisional interactions. Therefore, coherent color fields are less effective for heavy-quark energy loss than collisions.

- Secondly, κ_L and κ_T from color fields decrease with increasing heavy quark velocity, while those from collisions increase. The reason for decreasing diffusion coefficients in color fields is that the time during which a heavy quark remains in one domain of color field decreases with increasing heavy quark velocity, and the short stay reduces the correlation of the color Lorentz forces.

We have also found that the contribution from coherent color fields to heavy quark diffusion is important in the early stage of relativistic heavy-ion collisions, because κ_L and κ_T from color fields are proportional to ε and α_s, while those from collisions vary as $\varepsilon^{3/4}$ and α_s^2.

As our study is restricted to fast mid-rapidity heavy quarks, it would be very interesting to extend to heavy quarks with small velocity or in forward and backward rapidities. For this one would a priori just need the correlation length of coherent color fields in the τ and η directions.

Acknowledgements

This work has been supported by DFG under contract BR 4000/3-1, by BMBF under project No. 05P12RFFCQ, by the LOEWE center "HIC for FAIR", and by the Natural Sciences and Engineering Research Council of Canada (NSERC). The computational resources have been provided by the LOEWE-CSC, as well as the Guillimin supercomputer at McGill University, managed by Calcul Québec and Compute Canada. The operation of this supercomputer is funded by the Canada Foundation for Innovation (CFI), Ministère de l'Economie, de l'Innovation et des Exportations du Québec (MEIE), RMGA and the Fonds de recherche du Québec - Nature et technologies (FRQ-NT).

Appendix A: electric and magnetic field equality for purely gluonic systems

To the best of our knowledge, the equality deduced at the end of this appendix has yet to be written somewhere. For completeness, let us roughly sketch its derivation. Starting from the Classical Yang-Mills equations written in a covariant form

$$\frac{1}{\sqrt{-g}} D_\mu^{ab} \left[\sqrt{-g} g^{\mu\alpha} g^{\nu\beta} F_{\alpha\beta}^b\right] = 0 \,, \tag{30}$$

where $g = \det g_{\mu\nu}$, the covariant derivative being defined from the gluonic fields as

$$D_\mu^{ab} = \delta^{ab}\partial_\mu - igA_\mu^{ab} \,, \tag{31}$$

and the Maxwell-stress tensor being

$$F_{\mu\nu}^a = \partial_\mu A_\nu^a - \partial_\nu A_\mu^a - ig[A_\mu, A_\nu]^a \,. \tag{32}$$

Placing ourselves in the Milne coordinate system

$$\tau = \sqrt{t^2 - z^2} \qquad \eta = \frac{1}{2}\ln\frac{t+z}{t-z} \,, \tag{33}$$

where the metric tensor reads

$$g_{\mu\nu} = \mathrm{diag}(1, -1, -1, -\tau^2) \tag{34}$$

and defining as is usually done in this coordinate system the electric fields as (here i runs on only on the transverse spatial coordinates x, y)

$$E^{ia} = \tau\partial_\tau A_i^a \qquad E^{\eta a} = \frac{1}{\tau}\partial_\tau A_\eta^a \,, \tag{35}$$

we get a constraint equation (Gauss's law) by picking $\nu = \tau$ in Eq. (30)

$$D_i E^i + D_\eta E^\eta = 0 \,, \tag{36}$$

and three equations for the time derivative of the transverse and longitudinal electric fields by picking$\nu = i, \eta$ in Eq. (30)

$$\partial_\tau E^{ia} = \tau D_j^{ab} F_{ji}^b + \frac{1}{\tau} D_\eta^{ab} F_{\eta i}^b \,, \quad \partial_\tau E^{\eta a} = \frac{1}{\tau} D_i^{ab} F_{i\eta}^b \,. \tag{37}$$

Deriving the constraint equation (36) trivially leads to

$$D_i^{ab}\partial_\tau E^{ib} + D_\eta^{ab}\partial_\tau E^{\eta b} - \frac{ig}{\tau} E^{ia} E^{ia} - ig\tau E^{\eta a} E^{\eta a} = 0 \,, \tag{38}$$

and using the following relation between the covariant derivative and the Maxwell-stress tensor

$$[D_\mu, D_\nu]^a = -igF^a_{\mu\nu} \ , \tag{39}$$

we get, by plugging Eq. (37) into Eq. (38)

$$\tau F^a_{xy}F^a_{xy} + \frac{1}{\tau}F^a_{i\eta}F^a_{i\eta} - \frac{1}{\tau}E^{ia}E^{ia} - \tau E^{\eta a}E^{\eta a} = 0 \ . \tag{40}$$

Finally, defining as usual the magnetic fields as

$$B^{\eta a} = F^a_{xy} \ , \qquad B^{xa} = F^a_{y\eta} \ , \qquad B^{ya} = F^a_{\eta x} \ , \tag{41}$$

we get

$$\tau B^{\eta a}B^{\eta a} + \frac{1}{\tau}B^{ia}B^{ia} = \frac{1}{\tau}E^{ia}E^{ia} + \tau E^{\eta a}E^{\eta a} \ . \tag{42}$$

Given the metric form in Milne coordinate system (34), one has

$$-E^a_\mu E^{\mu a} = E^{ia}E^{ia} + \tau^2 E^{\eta a}E^{\eta a} \ . \tag{43}$$

we therefore just proved that at all times (denoting the spatial indices $I = x, y, \eta$), the following equality relates the electric fields and the magnetic fields

$$E^a_I E^{Ia} = B^a_I B^{Ia} \ . \tag{44}$$

Appendix B: electric and magnetic field relations in the free-streaming case

Solving numerically the classical Yang-Mills equations [3], one finds that after some time

$$p_x \approx p_y \approx \frac{\epsilon}{2} \qquad\qquad p_z \approx 0 \ , \tag{45}$$

where, calling

$$\begin{aligned} E_x^2 &= \frac{E^a_x E^a_x}{\tau^2} \qquad E_y^2 = \frac{E^a_y E^a_y}{\tau^2} \qquad E_z^2 = E^a_\eta E^a_\eta \ , \\ B_x^2 &= \frac{B^a_x B^a_x}{\tau^2} \qquad B_y^2 = \frac{B^a_y B^a_y}{\tau^2} \qquad B_z^2 = B^a_\eta B^a_\eta \ , \end{aligned} \tag{46}$$

one has

$$\epsilon = \frac{1}{2}\left(E^2 + B^2\right) \ , \qquad p_i = \epsilon - E_i^2 - B_i^2 \ . \tag{47}$$

Given what we proved in the previous appendix, one has the additional relation valid at all times

$$E_x^2 + E_y^2 + E_z^2 = B_x^2 + B_y^2 + B_z^2 \ . \tag{48}$$

Equation (45) gives only two additional constraints on the fields :

$$E_z^2 + B_z^2 = E_x^2 + B_x^2 + E_y^2 + B_y^2 \ , \tag{49}$$

and

$$E_x^2 + B_x^2 = E_y^2 + B_y^2 \ . \tag{50}$$

Combining Eq. (48) with Eq. (49)-(50) leads to the following possible rewritting of the constraints

$$E_z^2 = B_x^2 + B_y^2 \qquad\qquad B_z^2 = E_x^2 + E_y^2 \ . \tag{51}$$

Making the additional assumptions (that seems reasonable after some time evolution, looking the numerical results of [3]) that

$$\begin{aligned} E_x^2 + E_y^2 &= B_x^2 + B_y^2 \\ E_z^2 &= B_z^2, \end{aligned} \tag{52}$$

we get

$$\begin{aligned} E_z^2 &= E_x^2 + E_y^2, \\ B_z^2 &= B_x^2 + B_y^2. \end{aligned} \tag{53}$$

[1] L. McLerran, Prog. Theor. Phys. Suppl. **187**, 17 (2011).
[2] G. Chen and R. J. Fries, Phys. Lett. B **723**, 417 (2013).
[3] T. Lappi and L. McLerran, Nucl. Phys. A **772**, 200 (2006).
[4] T. Epelbaum and F. Gelis, Phys. Rev. Lett. **111**, 232301 (2013).
[5] L. Adamczyk *et al.* [STAR Collaboration], Phys. Rev. Lett. **113**, 142301 (2014).
[6] D. Tlusty [STAR Collaboration], Nucl. Phys. A **904-905**, 639c (2013).
[7] B. Abelev *et al.* [ALICE Collaboration], JHEP **1209**, 112 (2012).
[8] B. Abelev *et al.* [ALICE Collaboration], Phys. Rev. Lett. **111**, 102301 (2013).
[9] M. Golam Mustafa, D. Pal and D. Kumar Srivastava, Phys. Rev. C **57**, 889 (1998) [Erratum-ibid. C **57**, 3499 (1998)].
[10] G. D. Moore and D. Teaney, Phys. Rev. C **71**, 064904 (2005).
[11] B. Zhang, L. W. Chen and C. M. Ko, Phys. Rev. C **72**, 024906 (2005).
[12] D. Molnar, Eur. Phys. J. C **49**, 181 (2007).
[13] H. van Hees, V. Greco and R. Rapp, Phys. Rev. C **73**, 034913 (2006).

[14] P. B. Gossiaux and J. Aichelin, Phys. Rev. C **78** 014904, (2008); P. B. Gossiaux, R. Bierkandt and J. Aichelin, Phys. Rev. C **79** 044906, (2009); J. Aichelin, P. B. Gossiaux and T. Gousset, Phys. Rev. D **89** 074018, (2014).
[15] M. Nahrgang, J. Aichelin, S. Bass, P. B. Gossiaux and K. Werner, Phys. Rev. C **91** (2015) 1, 014904.
[16] V. Ozvenchuk, J. M. Torres-Rincon, P. B. Gossiaux, L. Tolos and J. Aichelin, Phys. Rev. C **90**, 054909 (2014).
[17] S. Cao, G. Y. Qin and S. A. Bass, Phys. Rev. C **88**, 044907 (2013).
[18] W. M. Alberico, A. Beraudo, A. De Pace, A. Molinari, M. Monteno, M. Nardi and F. Prino, Eur. Phys. J. C **71**, 1666 (2011); *ibid* **73**, 2481 (2013).
[19] R. Sharma, I. Vitev and B. W. Zhang, Phys. Rev. C **80**, 054902 (2009).
[20]
[20] M. He, R. J. Fries and R. Rapp, Phys. Rev. C **86**, 014903 (2012); Phys. Rev. Lett. **110**, 112301 (2013).
[21] Y. Akamatsu, T. Hatsuda and T. Hirano, Phys. Rev. C **79**, 054907 (2009).
[22] J. Uphoff, O. Fochler, Z. Xu and C. Greiner, Nucl. Phys. A **910-911**, 401 (2013); *ibid* **931** (2014) 535.
[23] T. Lang, H. van Hees, J. Steinheimer and M. Bleicher, arXiv:1208.1643 [hep-ph].
[24] H. Berrehrah, P. B. Gossiaux, J. Aichelin, W. Cassing and E. Bratkovskaya, Phys. Rev. C **90**, no. 6, 064906 (2014).
[25] H. Berrehrah, P. B. Gossiaux, J. Aichelin, W. Cassing, J. M. Torres-Rincon and E. Bratkovskaya, Phys. Rev. C **90**, no. 5, 051901 (2014).
[26] H. Berrehrah, E. Bratkovskaya, W. Cassing, P. B. Gossiaux and J. Aichelin, Phys. Rev. C **91**, no. 5, 054902 (2015).
[27] S. K. Das, F. Scardina, S. Plumari and V. Greco, Phys. Rev. C **90**, 044901 (2014).
[28] S. K. Das, F. Scardina, S. Plumari and V. Greco, Phys. Lett. B **747**, 260 (2015).
[29] T. Song, H. Berrehrah, D. Cabrera, J. M. Torres-Rincon, L. Tolos, W. Cassing and E. Bratkovskaya, Phys. Rev. C **92**, no. 1, 014910 (2015).
[30] M. Asakawa, S. A. Bass, B. Muller, Prog. Theor. Phys. **116**, 725-755 (2007).
[31] A. Majumder, B. Muller and S. A. Bass, Phys. Rev. Lett. **99**, 042301 (2007).
[32] D. F. Litim and C. Manuel, Phys. Rept. **364**, 451 (2002).
[33]
[33] E. Iancu and R. Venugopalan, In *Hwa, R.C. (ed.) et al.: Quark gluon plasma* 249-3363
[34] M. Cacciari, P. Nason and R. Vogt, Phys. Rev. Lett. **95** (2005) 122001.
[35] T. Song, W. Park and S. H. Lee, Phys. Rev. C **84**, 054903 (2011).
[36] T. Song, K. C. Han and C. M. Ko, Nucl. Phys. A **897**, 141 (2013).